New Journal of Chemistry

Electronic Supporting Information (ESI) for

An easy synthetic access to new pyrazole spiro derivatives from 3-amino-1-phenyl-2-pyrazolin-5-one

Jamila Zaiter[a], Hanane Achibat[a], Ouafa Amiri[a], Abderrafia Hafid[a], Mostafa Khouili[a,*], El Mostapha Rakib[a], Cláudia M. B. Neves[b], Maria Graça P. M. S. Neves[b], Artur M. S. Silva[b], José A. S. Cavaleiro[b], Filipe A. Almeida Paz[c], Maria A. F. Faustino[b,*]

[a]Laboratoire de Chimie Organique & Analytique, Université Sultan Moulay Slimane, Faculté des Sciences et Techniques, BP 523, 23000 Béni-Mellal, Morocco,

[b]Department of Chemistry and QOPNA, University of Aveiro, 3810-193 Aveiro, Portugal and

[c]Department of Chemistry, CICECO – Aveiro Institute of Materials, University of Aveiro, 3810-193 Aveiro, Portugal

* Corresponding authors. *E-mail addresses*: Mostafa Khouili - m.khouili@usms.ma and Maria Amparo Ferreira Faustino – faustino@ua.pt

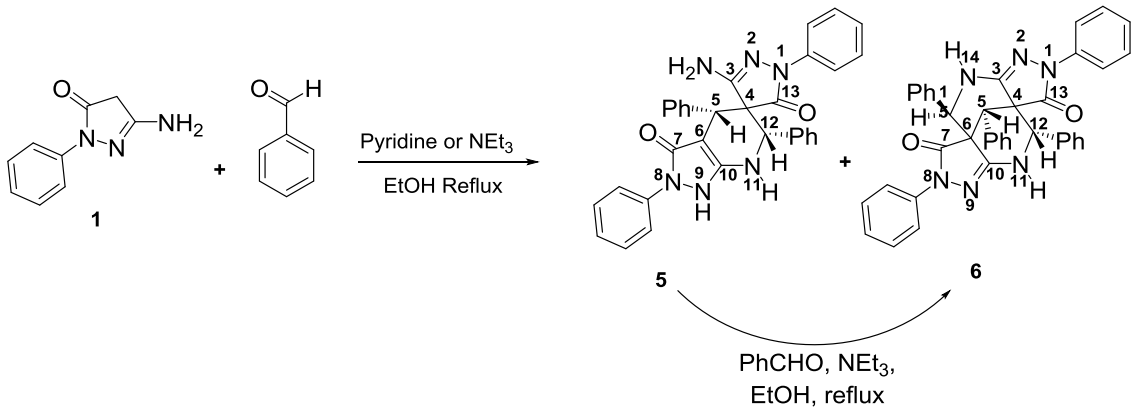

Table of Contents

I. General remarks

All the chemicals were purchased from commercial sources and were used without any further purification. The reactions were monitored by thin layer chromatography TLC and the spots were examined under UV light at λ = 254 and 365 nm.

Compounds were characterized by ^{1}H and ^{13}C NMR spectra using $CDCl_3$ or $CDCl_3/CD_3OD$ as solvent and tetramethylsilane (TMS) as internal reference. ^{1}H and ^{13}C NMR spectra were recorded on a Bruker Avance 300 spectrometer at 300.13 and 75.47 MHz, respectively. The chemical shifts are reported in δ (ppm) and the coupling constants (*J*) in hertz (Hz). The electrospray mass spectrometry (ESI-MS) spectra in positive ion mode were acquired in a Q-TOF 2 instrument (Micromass, Manchester, UK). For the acquisition of mass spectra the needle voltage was set at 3000 V with the ion source at 80 ºC and cone voltage at 30 V. The elemental analyses were obtained with a LECO 630-200-200 TruSpec CHNS Micro analyzer.

The melting points were determined with a Büchi melting point apparatus and are uncorrected.

II. Copies of ESI-MS and NMR spectra charts

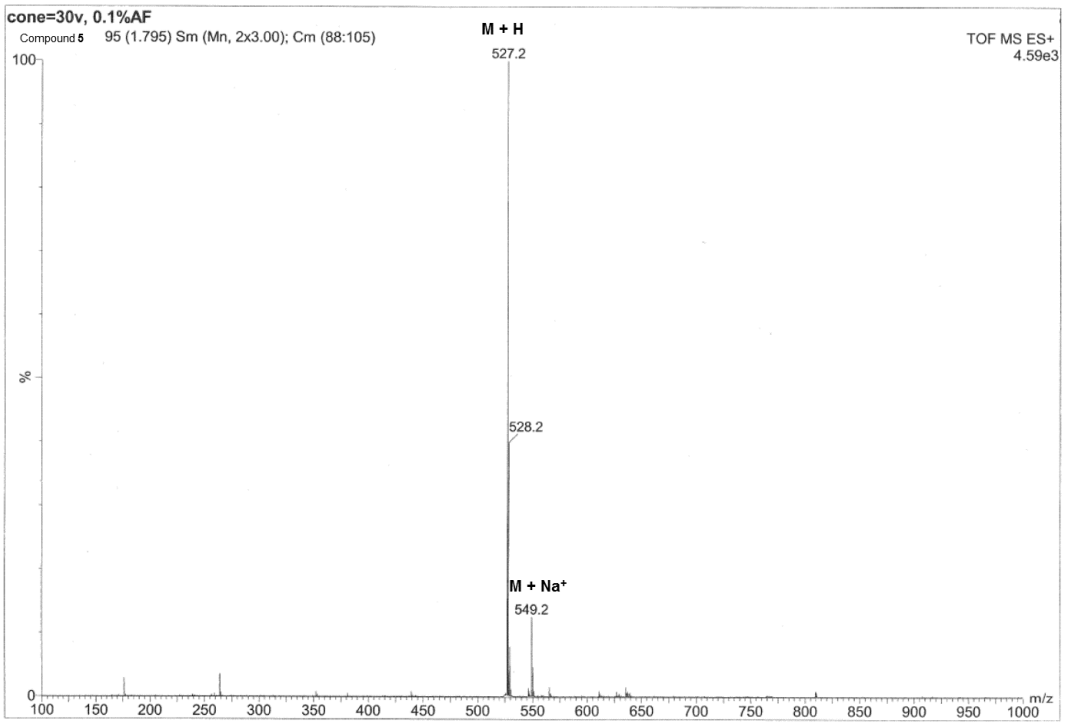

Figure S1. Electrospray mass spectra (ESI-MS) of compound **5**.

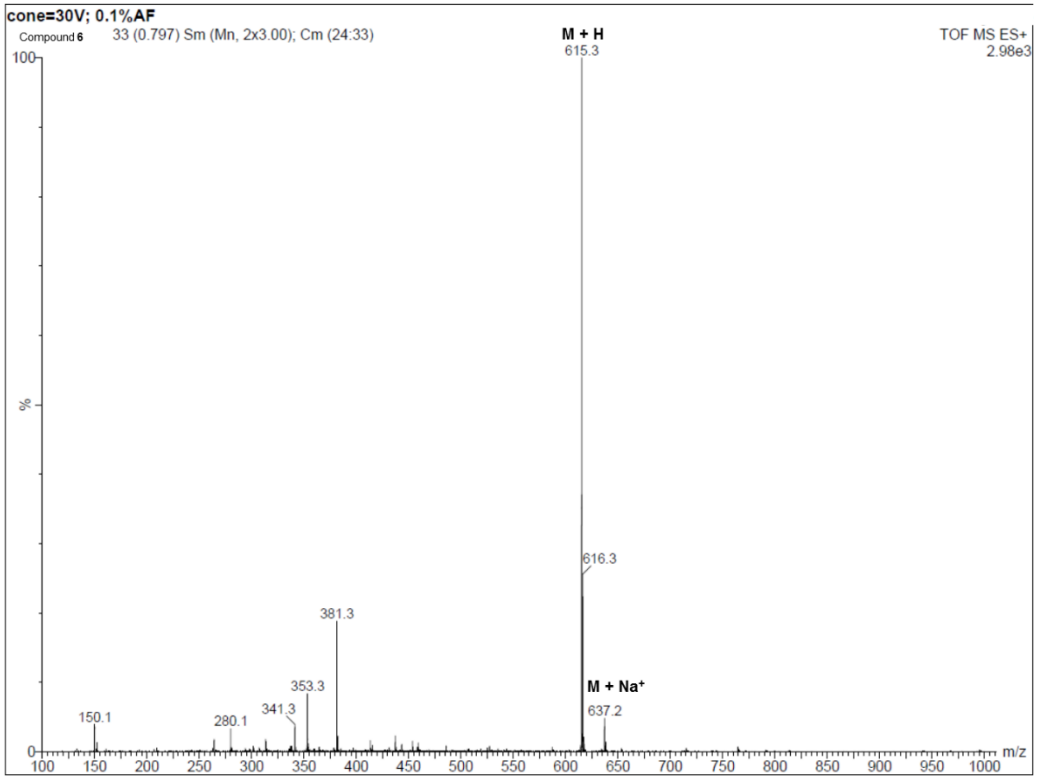

Figure S2. Electrospray mass spectra (ESI-MS) of compound **6**.

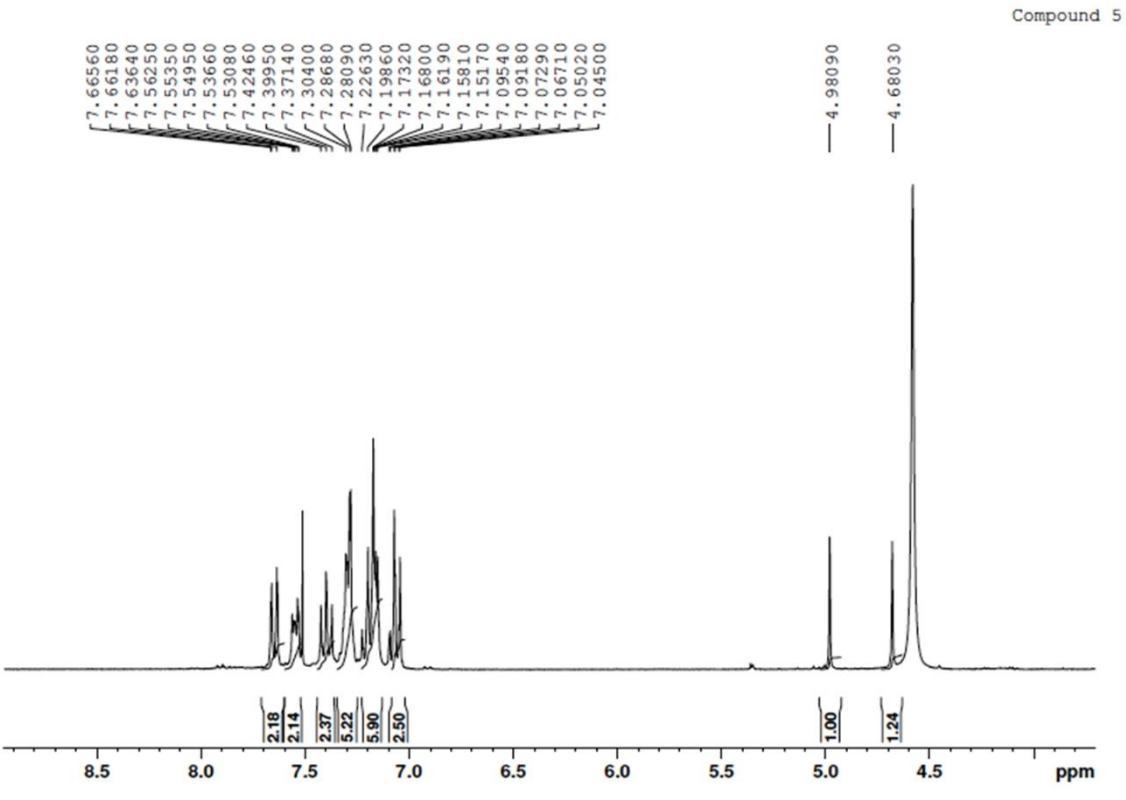

Figure S3. ^{1}H NMR spectrum of compound **5** using $CDCl_3/CD_3OD$ as solvent.

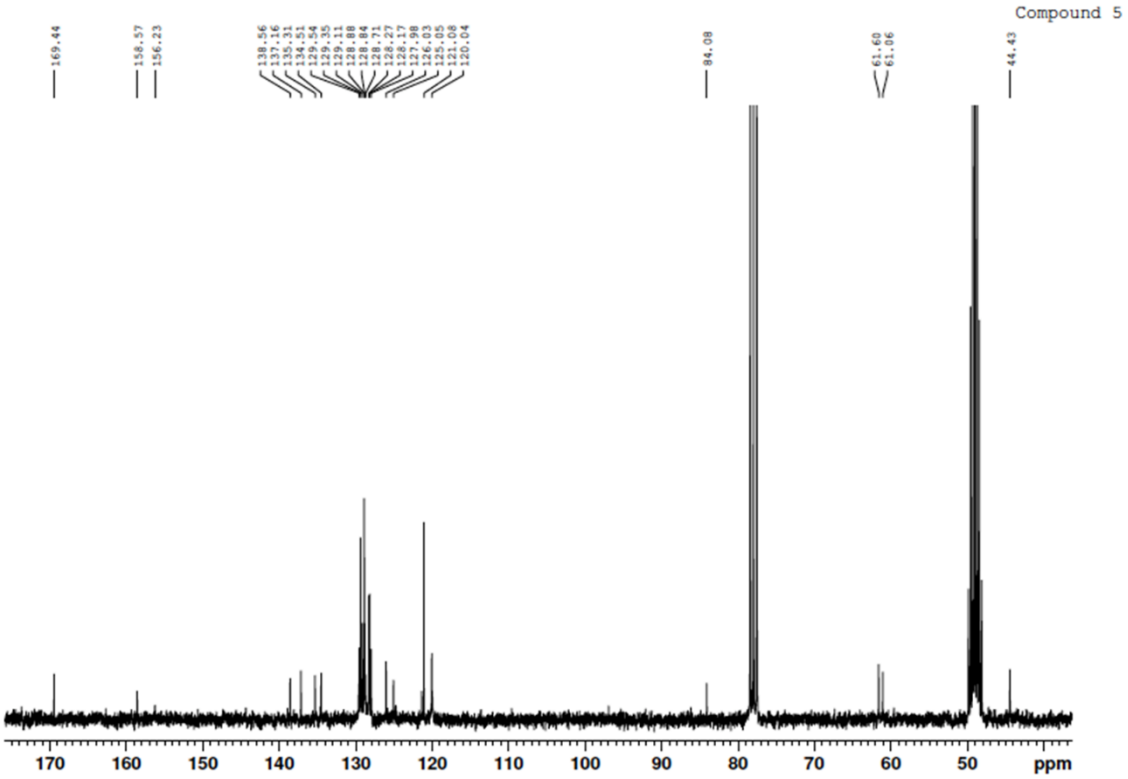

Figure S4. ^{13}C NMR spectrum of compound **5** using $CDCl_3/CD_3OD$ as solvent.

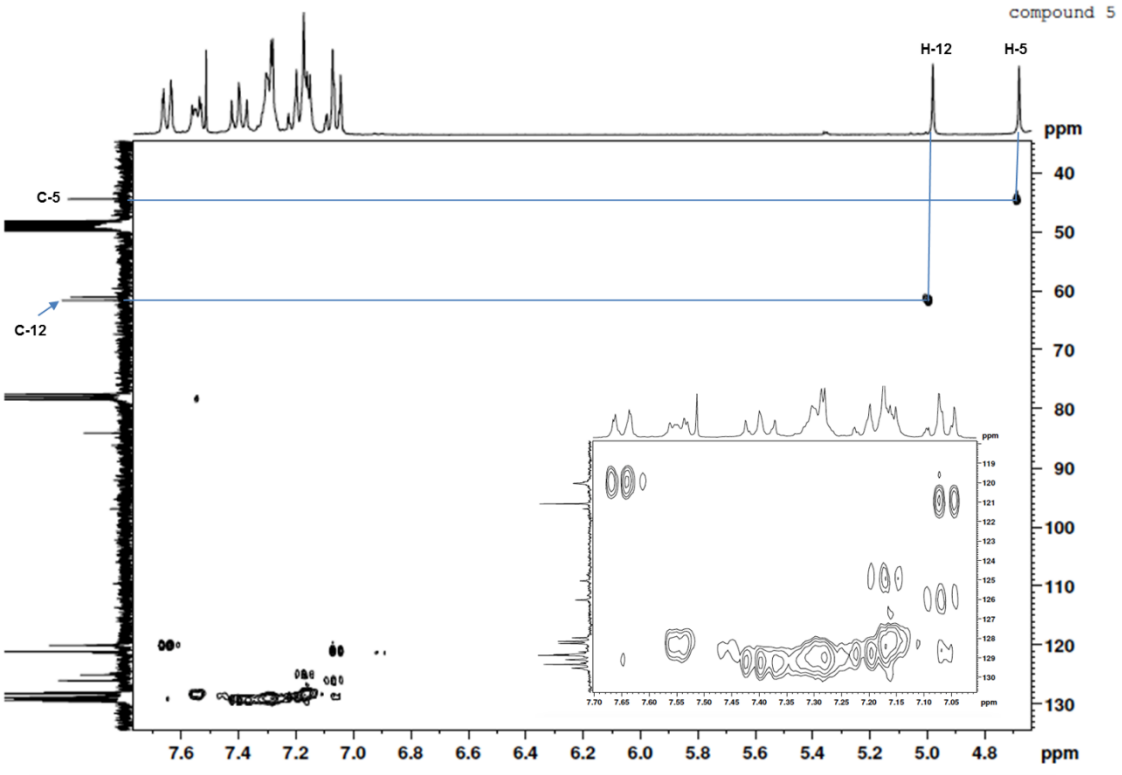

Figure S5. HSQC ($^{1}H/^{13}C$) spectrum of compound **5**.

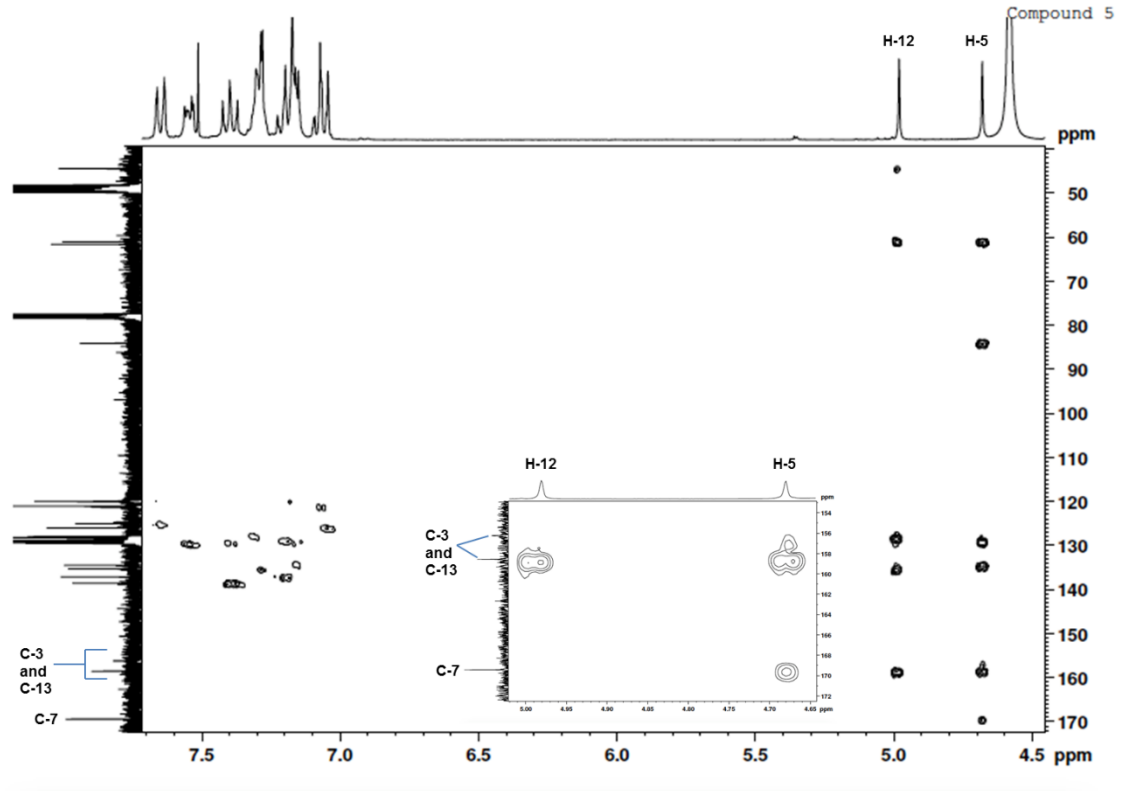

Figure S6. HMBC ($^{1}H/^{13}C$) spectrum of compound **5**.

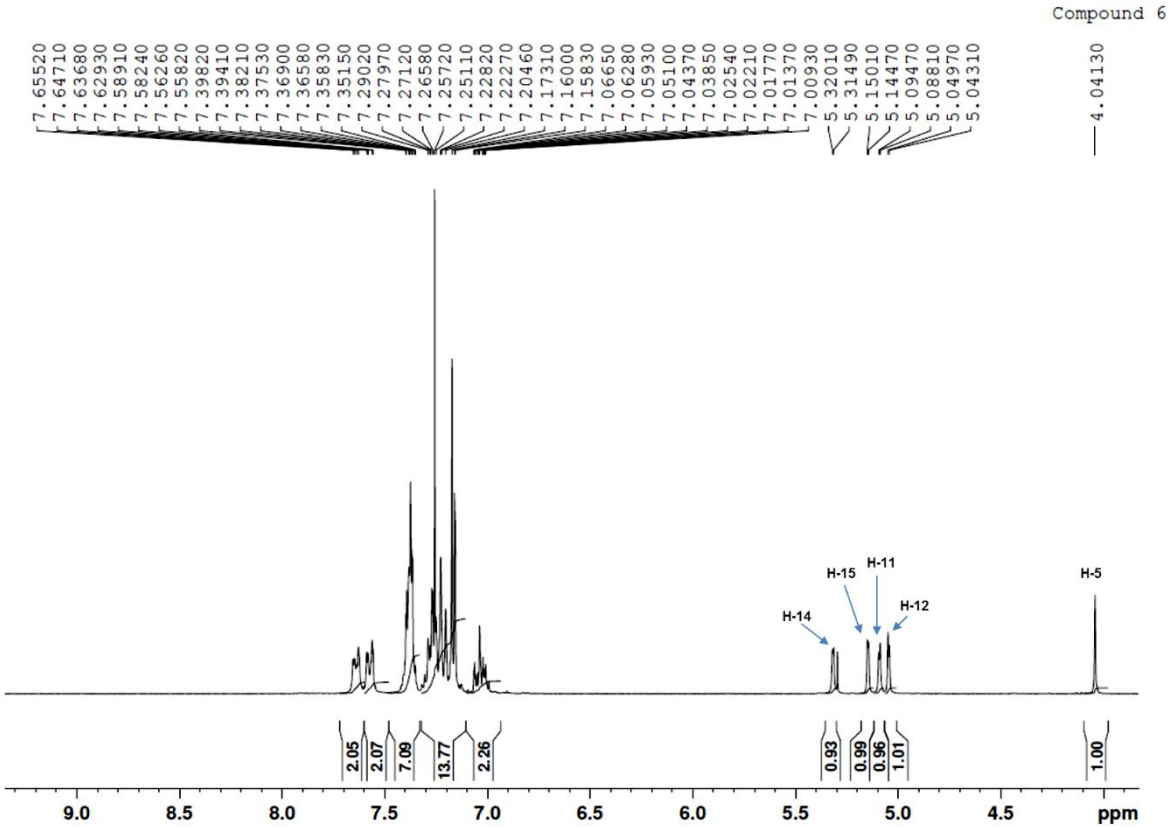

Figure S7. ^{1}H NMR spectrum of compound **6** using $CDCl_3$ as solvent.

Figure S8. COSY ($^{1}H/^{1}H$) spectrum of compound **6**.

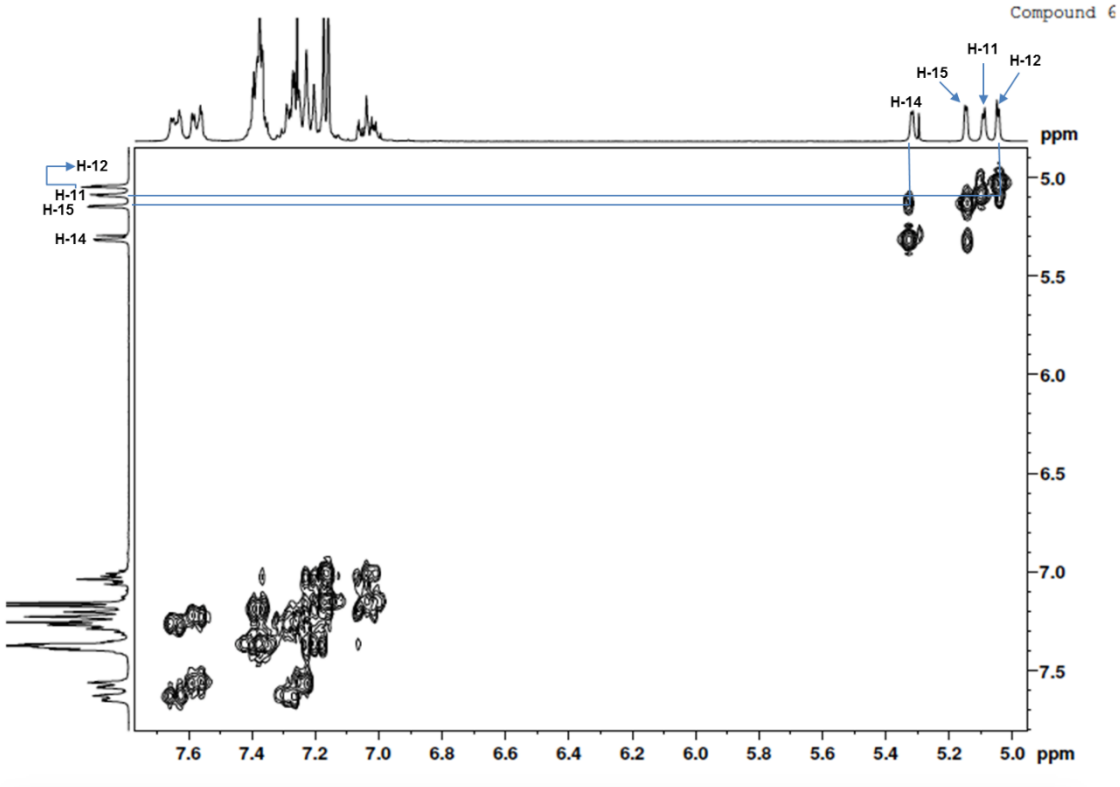

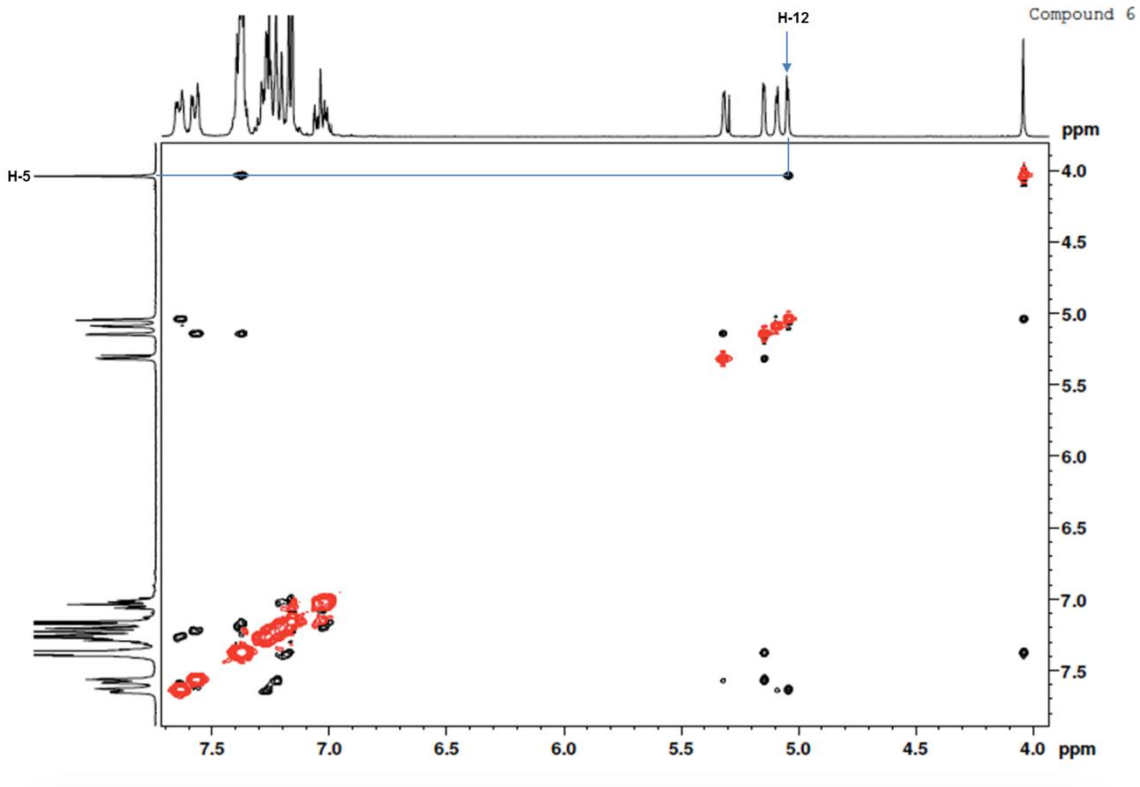

Figure S9. NOESY (^{1}H/^{1}H) spectrum of compound **6**.

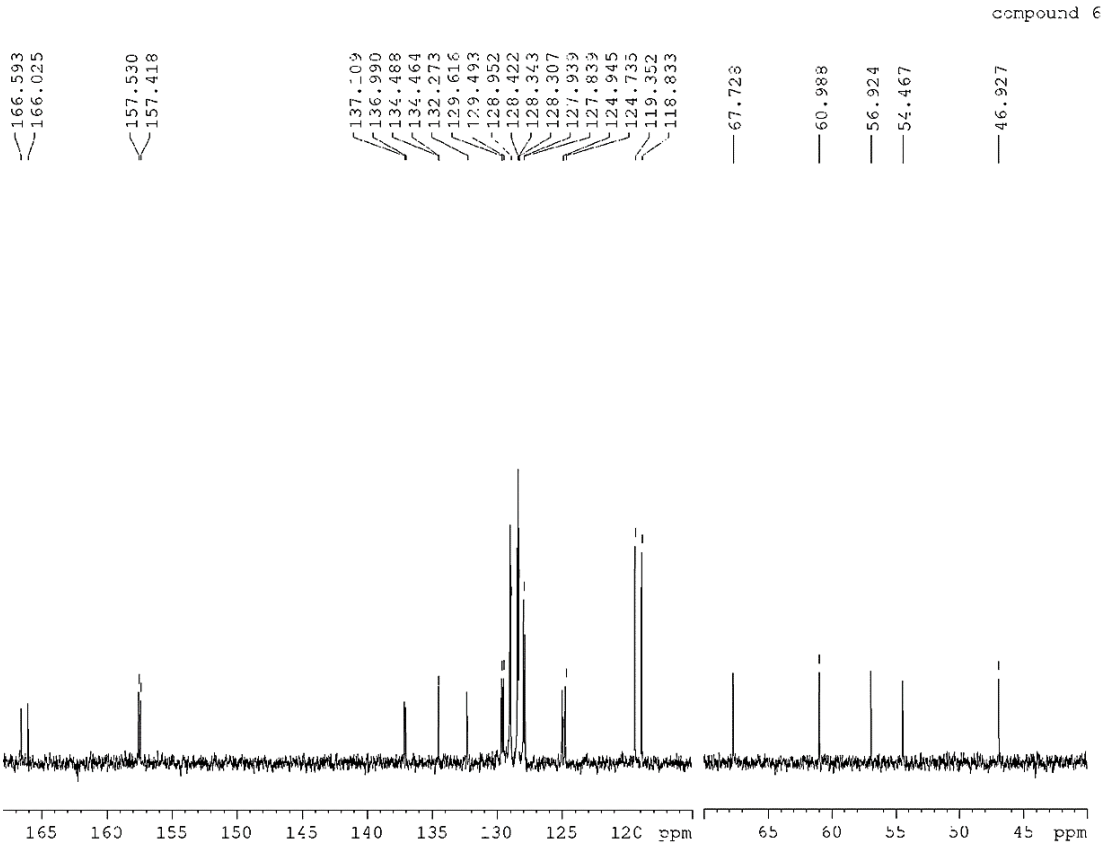

Figure S10. ^{13}C NMR spectrum of compound **6** using $CDCl_3$ as solvent.

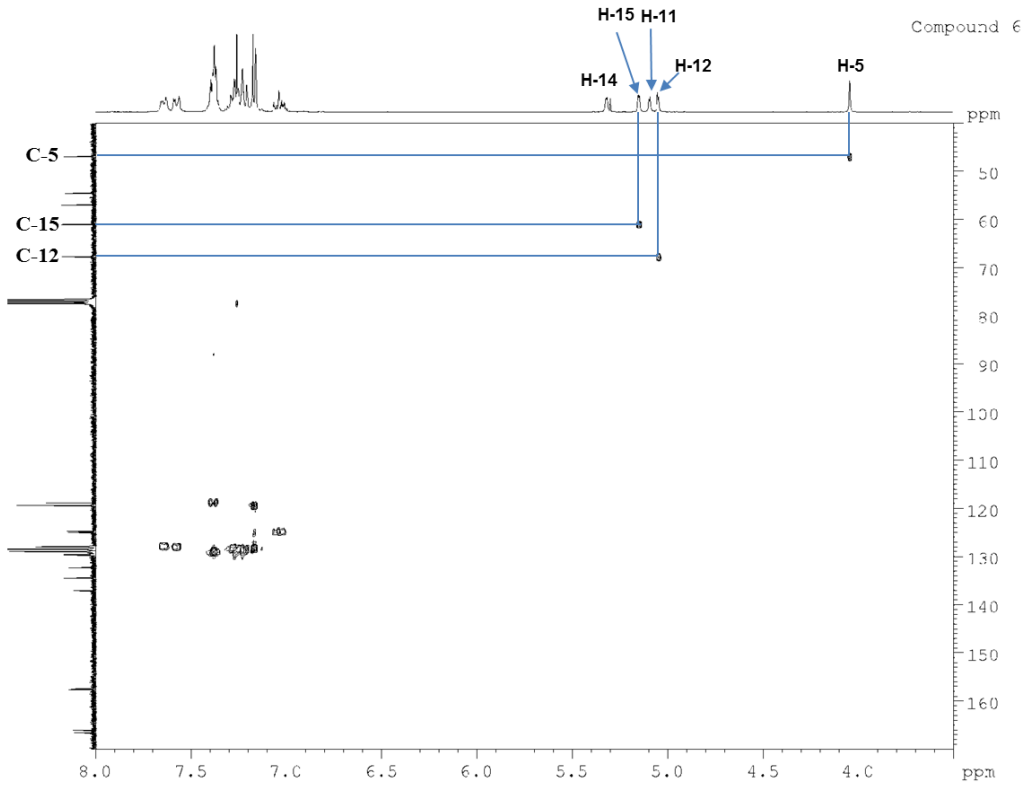

Figure S11. HSQC ($^{1}H/^{13}C$) spectrum of compound **6**.

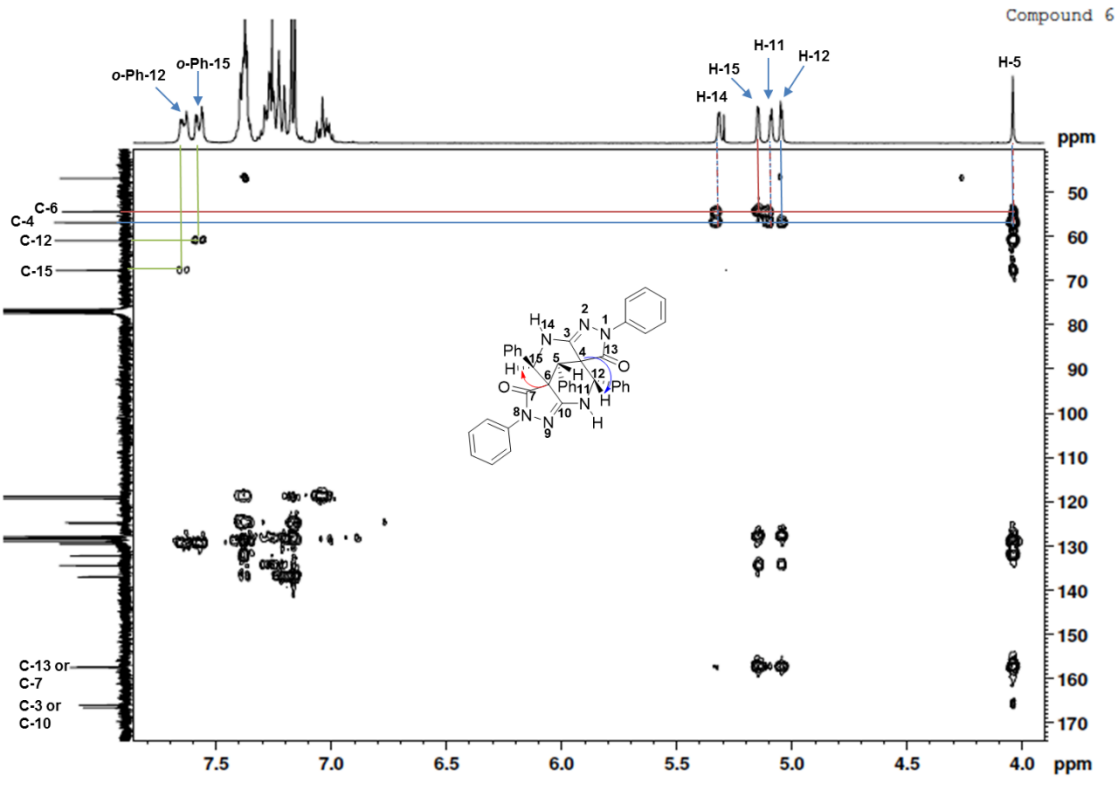

Figure S12. HMBC ($^{1}H/^{13}C$) spectrum of compound **6**.

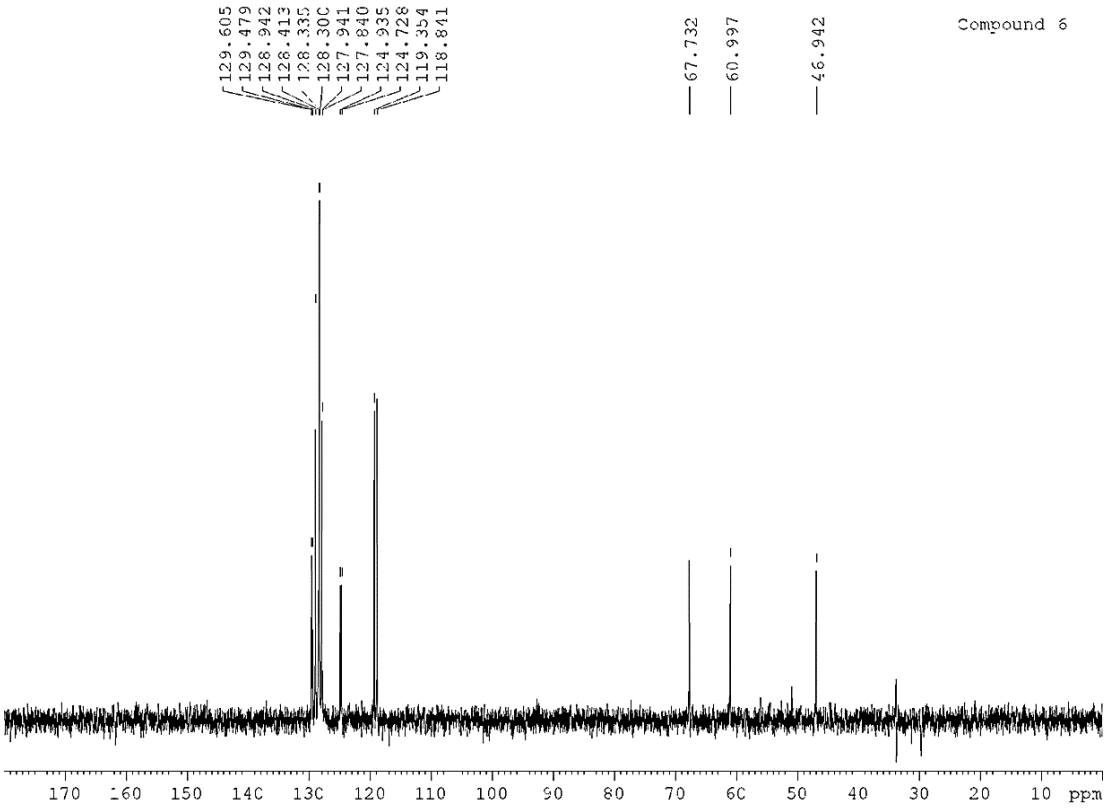

Figure S13. DEPT 135 spectrum of compound **6**.

III. Single-Crystal X-ray Diffraction Studies

Single crystals of compound **5** were manually harvested from the crystallization vial and immersed in highly viscous FOMBLIN Y perfluoropolyether vacuum oil (LVAC 140/13, Sigma-Aldrich) to avoid degradation caused by the evaporation of the solvent [1]. Crystals were mounted on a Hampton Research CryoLoop with the help of a Stemi 2000 stereomicroscope equipped with Carl Zeiss lenses. Data were collected on a Bruker X8 Kappa APEX II CCD area-detector diffractometer (Mo Kα graphite-monochromated radiation, λ = 0.71073 Å) controlled by the APEX2 software package [2] and equipped with an Oxford Cryosystems Series 700 cryostream monitored remotely using the software interface Cryopad [3]. Images were processed using the software package SAINT+ [4], and data were corrected for absorption by the multiscan semi-empirical method implemented in SADABS [5]. The structure was solved using the algorithm implemented in SHELXT-2014 [6], which allowed the immediate location of almost all of the heaviest atoms composing the molecular unit of the two compounds. The remaining missing non-hydrogen atoms were located from difference Fourier maps calculated from successive full-matrix least-squares refinement cycles on F^2 using the latest SHELXL from the 2014 release [7,8]. All structural refinements were performed using the graphical interface ShelXle [9]. All non-hydrogen atoms present in the crystal structure could be successfully refined by assuming anisotropic displacement parameters.

The crystal diffracted poorly throughout the entire angular range. Indeed, below *ca.* 1.16 Å of resolution the R_{int} value is systematically very high (*i.e.*, above *ca.* 0.10). The poor quality of the overall diffraction has important consequences in the modeled structure, giving also rise to a number of alerts in PLATON [10,11]. Nevertheless, structure solution showed immediately the presence of the two most important chemical moieties in the crystal structure of **5**: the pair of *S*,*R*,*S* and *R*,*S*,*R* enantiomers (see Figure S14). Besides these molecules, five and two crystallographically independent, but partially-occupied, chloroform and acetone solvent molecules, respectively, were also located from difference Fourier maps. These solvent molecules add up to a total of respectively, 3.5 and 0.5 per pair of enantiomers. These solvent molecules were included in the final structural model with the internal bond distances restrained in order to ensure a chemically reasonable geometry for these entities.

The *R*,*S*,*R* enantiomer was found to exhibit a considerable structural disorder for a portion of the molecule as depicted in Figure S14b: one phenyl group was modelled

over three distinct crystallographic positions for which the use of the *AFIX 66* instruction in SHELXL was required in order to maintain a chemically reasonable geometry for each position.

All hydrogen atoms associated with nitrogen were directly located from difference Fourier maps and were included in the final structural model with the N–H distances restrained to 0.95(1) Å. For the amino groups the H···H distance was further restrained to 1.55(1) Å in order to ensure a chemically reasonable geometry for these moieties. The isotropic thermal displacements parameters (U_{iso}) of these hydrogen atoms were fixed at 1.5×U_{eq} of the parent nitrogen atoms. Hydrogen atoms bound to carbon were placed instead at their idealized positions using the *HFIX 43* (aromatic carbon atoms) or *13* (tertiary carbon atoms) instructions in SHELXL. These hydrogen atoms were included in subsequent refinement cycles with isotropic thermal displacements parameters (U_{iso}) fixed at 1.2×U_{eq} of the parent carbon atoms.

The last difference Fourier map synthesis showed the highest peak (0.968 eÅ^{-3}) and the deepest hole (-0.690 eÅ^{-3}) located at 0.93 and 0.53 Å from H850 and Cl6S, respectively

Information concerning crystallographic data collection and structure refinement details is summarized in Table S1. Table S2 lists the most structurally relevant and strong supramolecular contacts present in the crystal structure of compound **5**. Structural drawings have been created using the software package Crystal Impact Diamond [12].

Crystallographic data (including structure factors) for the crystal structure of compound **5** have been deposited with the Cambridge Crystallographic Data Centre as supplementary publication No. CCDC- 1031778. Copies of the data can be obtained free of charge on application to CCDC, 12 Union Road, Cambridge CB2 2EZ, U.K. FAX: (+44) 1223 336033. E-mail: deposit@ccdc.cam.ac.uk.

Table S1. Crystal and structure refinement data for compound **5**

Formula	$C_{69}H_{58.5}Cl_{10.5}N_{12}O_{4.50}$
Formula weight	1500.00
Crystal system	Triclinic
Space group	*P*$\bar{1}$
a/Å	11.4963(12)
b/Å	16.0196(17)
c/Å	20.763(2)
α / º	78.971(4)
β / º	85.227(5)
γ / º	81.247(4)
Volume/Å^3	3703.7(7)
Z	2
D_c/g cm^{-3}	1.345
μ(Mo-Kα)/mm^{-1}	0.450
Crystal size/mm	0.12×0.07×0.02
Crystal type	Colourless plates
θ range	3.57 to 25.35
Index ranges	$-13 \le h \le 13$
	$-19 \le k \le 19$
	$-25 \le l \le 25$
Reflections collected	78963
Independent reflections	13499 [R_{int} = 0.0689]
Completeness to θ = 25.24°	99.5%
Final *R* indices [I>2σ(I)][a,b]	*R*1 = 0.0812
	*wR*2 = 0.2063
Final *R* indices (all data)[a,b]	*R*1 = 0.1132
	*wR*2 = 0.2254
Weighting scheme[c]	*m* = 0.1127
	n = 5.2229
Largest diff. peak and hole	0.968 and -0.690 eÅ^{-3}

[a] $R1 = \sum \| |F_o| - |F_c| \| / \sum |F_o|$; [b] $wR2 = \sqrt{\sum \left[w\left(F_o^2 - F_c^2\right)^2 \right] / \sum \left[w\left(F_o^2\right)^2 \right]}$

[c] $w = 1/\left[\sigma^2\left(F_o^2\right) + \left(mP\right)^2 + nP \right]$ where $P = \left(F_o^2 + 2F_c^2\right)/3$

Table S2. Geometrical details (distances in Å and angles in degrees) on the strong hydrogen bonds present in compound **5**.[a]

D–H···A	***d*(D···A)**	**<(DHA)**
N2−H1···O3^{i}	2.655(3)	138
N3−H3···O3^{i}	2.908(4)	142
N8−H8···O1	2.786(4)	134
N8−H8···O600^{ii}	2.989(9)	142
N9−H9···O1	2.736(3)	143
N12−H12B···N11^{iii}	2.966(9)	170
N12−H12B···N11'^{iii}	2.99(2)	165
N12−H12C···O301^{iv}	2.963(12)	141

[a] Symmetry transformations used to generate equivalent atoms:
(i) -1+*x*, *y*, *z*; (ii) 1-*x*, -*y*, 1-*z*; (iii) 2-*x*, -*y*, -*z*; (iv) 1+*x*, -1+*y*, *z*.

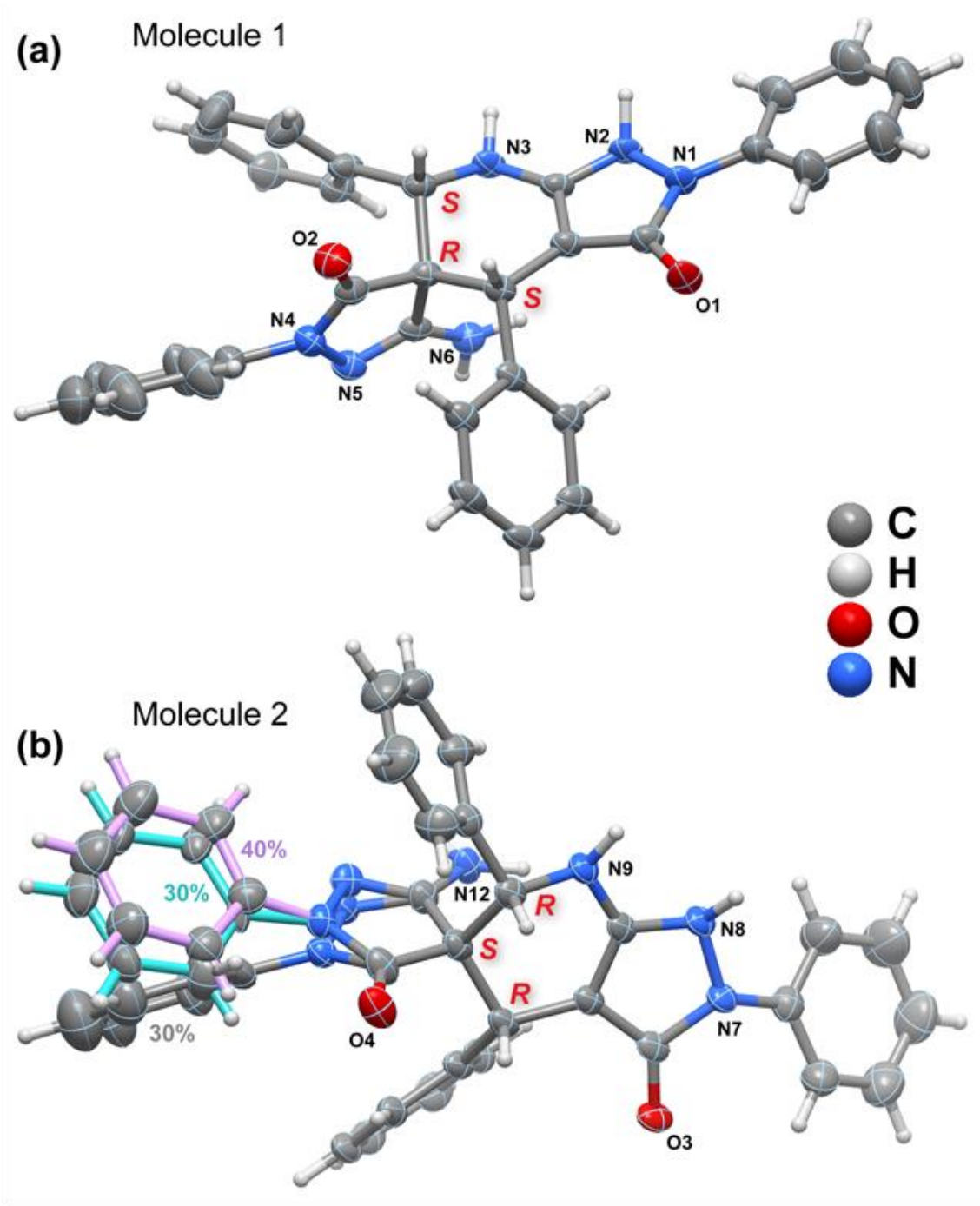

Figure S14. Schematic representation of the pair of enantiomers composing the asymmetric unit of compound **5**. Non-hydrogen atoms are represented as thermal ellipsoids drawn at the 50% probability level and hydrogen atoms are depicted as small spheres with arbitrary radii. The atomic labelling for the heteroatoms (*i.e.*, those involved in the strong supramolecular interactions present in the crystal structure – see Figures S15 and S16) is also depicted.

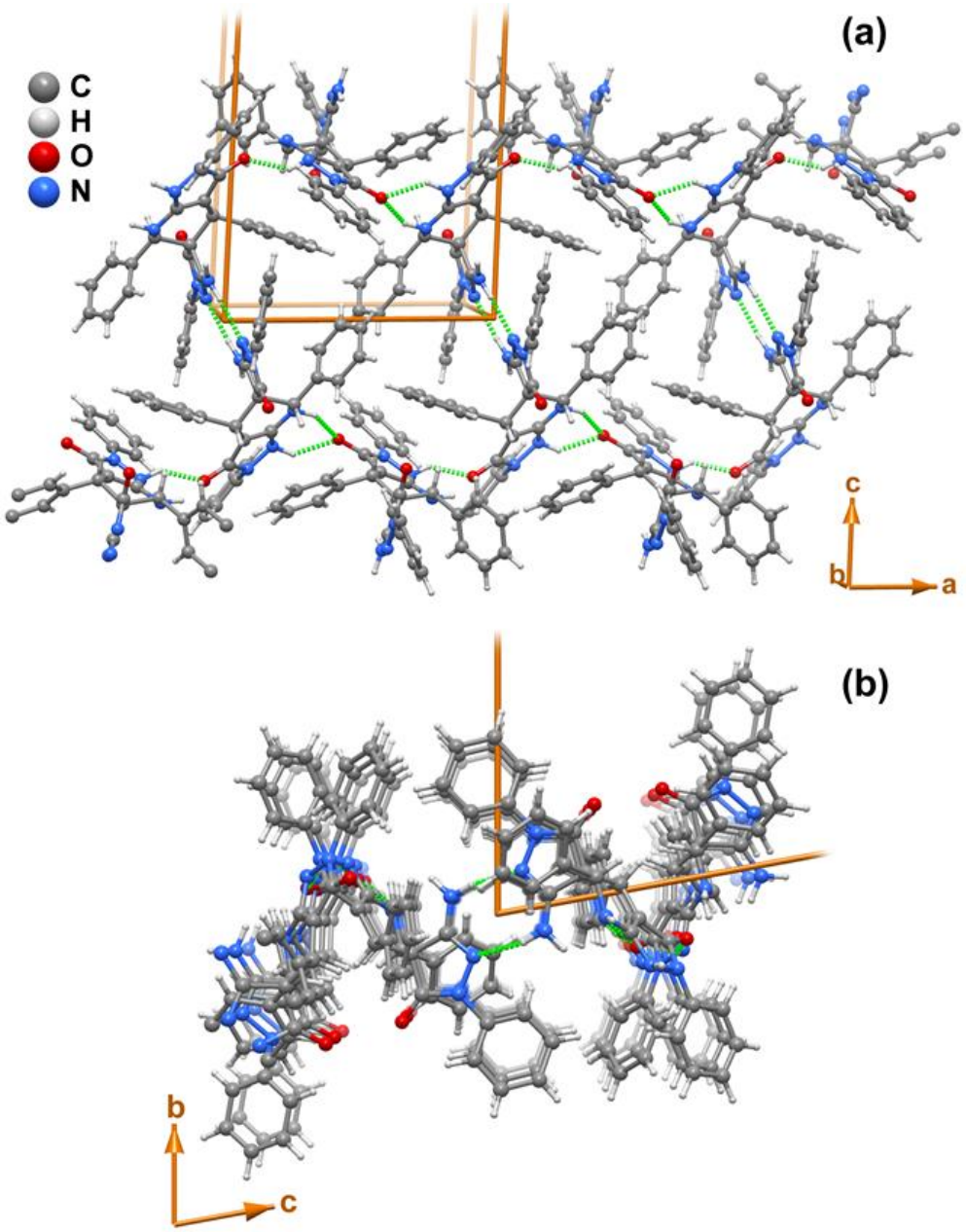

Figure S15. Schematic representation of the chain of strong N−H···(N,O) hydrogen bonds running parallel to the *a*-axis of the unit cell, promoting the interconnection of adjacent pairs of enantiomers in compound **5**. For geometrical details on the represented supramolecular interactions see Table S2. *Please note*: for the disordered molecules only the component with the highest occupancy factor has been represented for the sake of clarity.

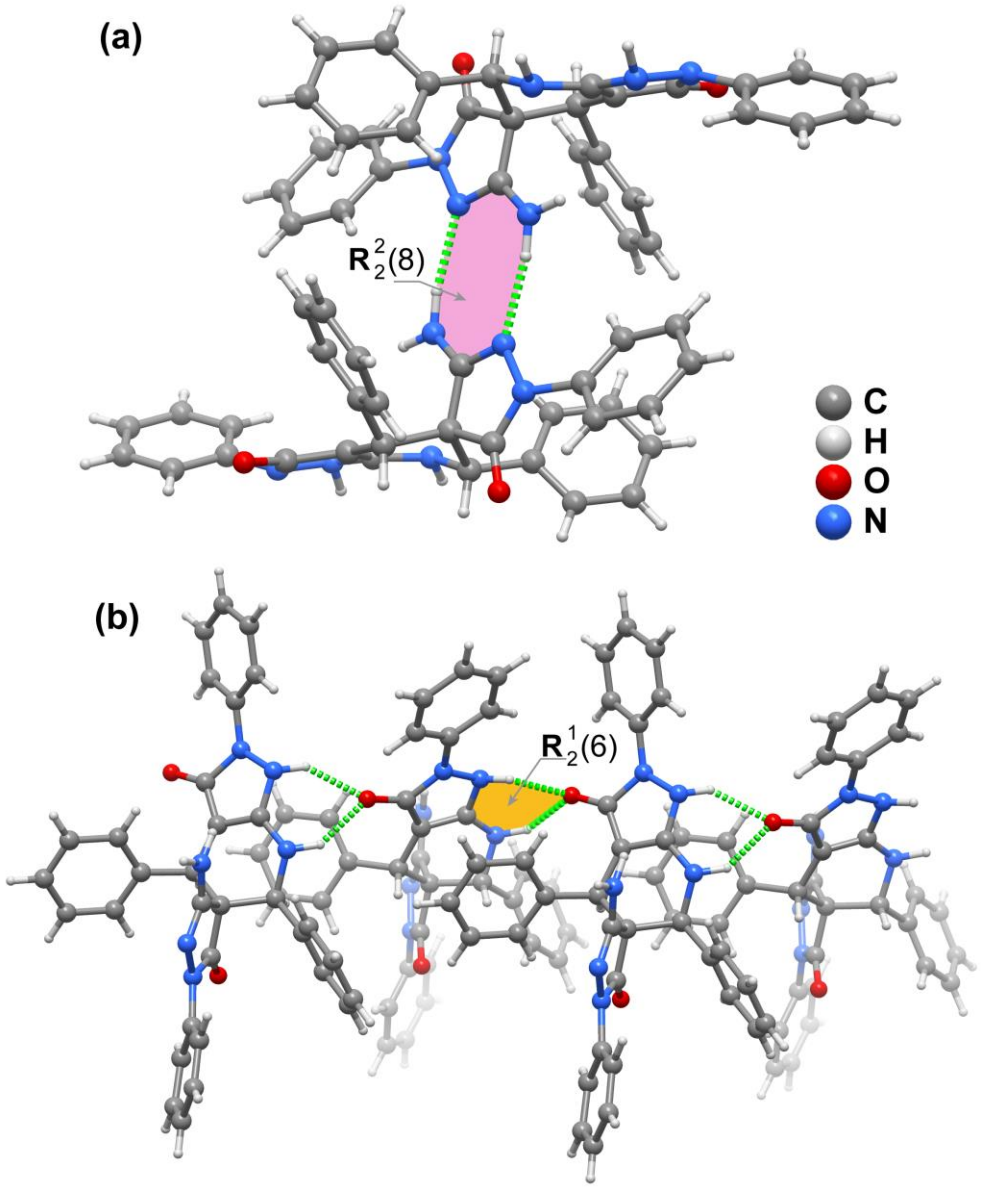

Figure S16. Detailed view of the two graph set motifs [13] interconnecting adjacent pairs of enantiomers in compound **5**: **(a)** $\mathbf{R}^2_2(8)$ and **(b)** $\mathbf{R}^1_2(6)$. For geometrical details on the represented supramolecular interactions see Table S2. *Please note*: for the disordered molecules only the component with the highest occupancy factor has been represented for the sake of clarity.

VI. References

[1] Kottke, T.; Stalke, D. *J. Appl. Crystallogr.* **1993,** *26*, 615-619.

[2] APEX2. *Data Collection Software Version 2.1-RC13, Bruker AXS, Delft, The Netherlands* **2006**.

[3] Cryopad. *Remote monitoring and control, Version 1.451, Oxford Cryosystems, Oxford, United Kingdom* **2006**.

[4] SAINT+. *Data Integration Engine v. 8.27b*© **1997-2012**, Bruker AXS, Madison, Wisconsin, USA.

[5] Sheldrick, G. M. *SADABS 2012/1, Bruker AXS Area Detector Scaling and Absorption Correction* **2012**, Bruker AXS, Madison, Wisconsin, USA.

[6] Sheldrick, G. M. *SHELXT-2014, Program for Crystal Structure Solution, University of Göttingen* **2014**.

[7] (a) Sheldrick, G. M. *SHELXL Version 2014, Program for Crystal Structure Refinement, University of Göttingen* **2014**.

[8] Sheldrick, G. M. *Acta Cryst. A* **2008,** *64*, 112-122.

[9] Hübschle, C. B.; Sheldrick, G. M.; Dittric, B. *J. Appl. Crystallogr.* **2011,** *44*, 1281-1284.

[10] Spek, A. L. *J. Appl. Crystallogr.* **2003,** *36*, 7-13.

[11] Spek, A. L. *Acta Cryst. A* **1990,** *46*, C34.

[12] Brandenburg, K. *DIAMOND, Version 3.2f. Crystal Impact GbR, Bonn, Germany* **1997-2010**.

[13] Grell, J.; Bernstein, J.; Tinhofer, G. *Acta Cryst. B* **1999,** *55*, 1030-1043.